ELSEVIER

Journal of Power Sources 73 (1998) 127–145

JOURNAL OF POWER SOURCES

The Brite–EuRam lead-acid electric-vehicle battery project—progress report

A. Cooper *

Lead Development Association, 42 Weymouth Street, London W1N 3LQ, UK

Received 18 August 1997; accepted 20 December 1997

Abstract

As part of its first programme, the Advanced Lead-Acid Battery Consortium has a US$4.4 million project assisted by European Community funding. This was initiated by the European members of the Consortium under the Brite–EuRam programme. At the Sixth Asian Battery Conference, an interim report was given on progress on eight of the ten tasks and, now that the project is in its final year, most of these have been completed. The principal objective of the project was to incorporate the findings of this work into demonstration batteries. These would then be tested under the Eucar ECE-15 test regime and this part of the project is now well under way. This paper discusses the results of the research leading up to the design of the battery variants built for evaluation. It also attempts to identify the lessons which have been learnt from this complex programme involving 14 research partners as well as five additional financial sponsors.

Keywords: AGM separators; ALABC; Conductive additives; Curing and formation; Electro-osmotic promoters; Electric-vehicles; Gel batteries; Lead alloys; Lead-acid batteries

1. Background

The original research programme of the Advanced Lead-Acid Battery Consortium (ALABC) envisaged the spending of US$19.3 million raised, roughly equally, from industry and government sources to advance the performance of lead-acid electric-vehicle (EV) batteries. Accordingly, the European members of the Consortium grouped together to submit a proposal for funding under the Brite–EuRam research programme financed by the European Community. This was submitted in February 1993 and news of the success of the application was received in the following July. Following contract negotiations, the US$4.4 million project commenced on 1 January 1994 with the help of US$2.02 million from Brite–EuRam funds. The European participants in the project and their respective roles are shown in Table 1.

2. Project structure

The original work programme of the project envisaged the tasks being grouped into five categories. Of these, three would be carried out concurrently over the first 3 years of the programme. These are illustrated schematically in Fig. 1.

Following evaluation of the results in the earlier part of the programme, battery modules and complete EV batteries have been constructed for laboratory testing in conjunction with Eucar. Concurrent with this testing, another task is looking at the implications of any changes made for the recycling of these battery designs.

Within the five broad categories outlined in Fig. 1, the 10 research tasks planned are listed below, together with the organizations carrying out the work.

2.1. Category (a)

Task 1. Study of the effect of electronically conducting additives to the positive active material on the high-rate performance of lead-acid cells. Contractors: Varta and ZSW.

* Corresponding author.

0378-7753/98/$19.00

Table 1
European participants in the Brite–EuRam lead-acid EV project and their respective roles

Company	Country	Sponsor	Research
AEA Technology	UK		✓
Bitrode	UK	✓	
Britannia Refined Metals	UK	✓	
CMP Batteries	UK	✓	✓
Digatron	Germany	✓	
ENSC de Toulouse	France		✓
Entek International	UK	✓	✓
HJ Enthoven and Son	UK	✓	
FIAMM	Italy	✓	✓
Hagen Batterie	Germany	✓	✓
Hawker Batterie	UK	✓	✓
Metaleurop Recherche	France	✓	✓
Renault (Eucar)	France	✓	✓
Rheinische Zink	Germany	✓	
University of Kassel	Germany		✓
University of Nancy	France		✓
Varta Batterie	Germany	✓	✓
ZSW	Germany		✓

Task 2. Examination of the electro-osmotic capacity enhancement of lead-acid EV batteries. Contractors: CMP Batteries and AEA Technology.

Task 3. Evaluation of positive active material enhancement by the addition of conducting titanium sub-oxides in pasted-plate batteries. Contractor: Hawker Batteries.

2.2. Category (b)

Task 4. Improvement of cycle life under EV discharge and recharge conditions. Contractors: Varta and University of Kassel.

Task 5. Influence of curing and formation parameters on cycling behaviour at high discharge rates. Contractor: Hagen.

Task 7. Studies into the combined effect of the rate of discharge and the depth-of-discharge (DoD) on the cycle life of lead-acid EV batteries. Contractors: CMP (Sonnenschein) and ZSW.

2.3. Category (c)

Task 6. Separator optimization for valve-regulated lead-acid batteries for EV applications. Contractors: Hawker Batteries and Entek International.

Task 8. Examination of the effects of alloying elements on the mechanical properties, corrosion resistance and the passivation of positive grids. Contractors: Metaleurop Recherche, University of Nancy, CMP (CEAC) and ENSC de Toulouse.

2.4. Category (d)

Task 9. Manufacture and bench-testing of prototype, maintenance-free, advanced lead-acid batteries for EV applications. Contractors: FIAMM and Renault (Eucar).

2.5. Category (e)

Task 10. Development of recycling technology for advanced lead-acid EV batteries. Contractor: Hawker Batteries.

The main thrust of the programme of research has been to try and improve battery performance by increasing paste utilization and conductivity. In addition, specific initiatives

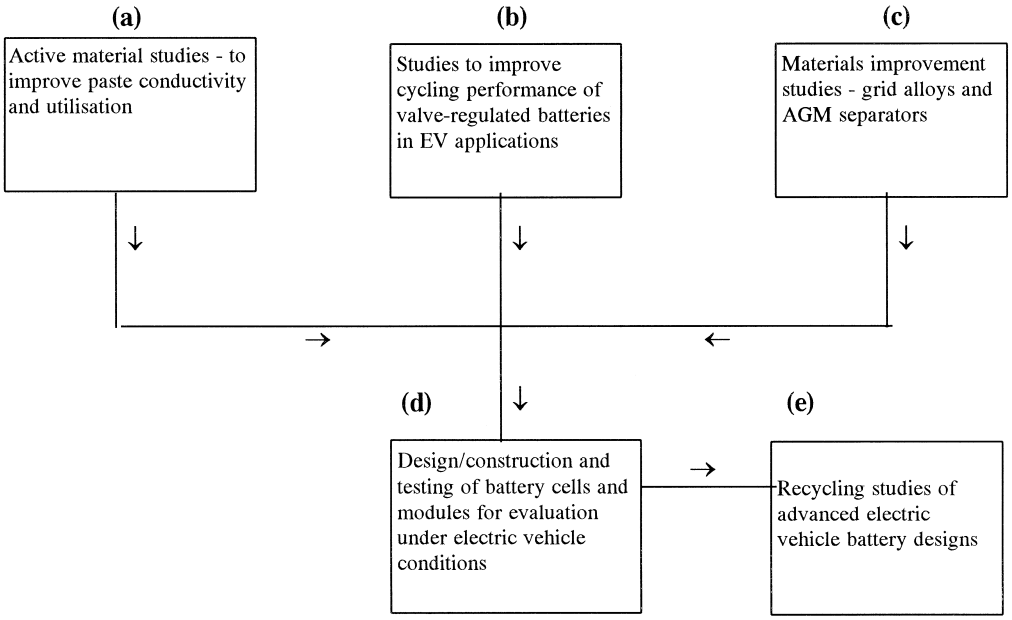

Fig. 1. Structure of Brite–EuRam EV project.

are aimed at improving battery life by investigating the phenomenon of premature capacity loss (PCL) and other factors detrimental to cycle life, as well as the formulation of improved battery alloys.

3. Project progress

As reported previously [1], most tasks started on schedule according to the agreed work programme, with the major exception of Task 3. Because of the difficulty in obtaining suitable high conductivity titanium sub-oxides in another ALABC programme, it was decided to substitute the original work in this Task with some work on the fast charging of EV batteries. This was not a duplication of other ALABC work, but set out to demonstrate the possibility of utilising a novel on-board charging system developed by Wavedriver in the UK. In this system, a compact power coupler acts as both the vehicle drive controller (converting dc power from the battery into ac for the traction motor) and also the charger (accepting ac line input and providing dc for recharge at high rates). The combined functions of the power coupler provide an economic approach to fast charging and has the potential to reduce significantly infra-structure cost.

Results from the various tasks can be summarized as follows.

Task 1: Conductive additives [2].

The goal of this work is to find and test positive-plate additives that can build up a conductive and chemically inert network in combination with lead dioxide. This should affect the mass utilization of modified active masses in model electrodes and commercial batteries to give higher specific capacity values. Considerations about the size, the shape and the amount of the conductive additive have also been made for optimized use. Ideally, these should have a high length-to-width (aspect) ratio as this shape is more effective in building up a conductive network than spherical particles. It has been found that the percolation threshold for a conductive fibre composite is reached at a fibre content of between 0.5 and 2.0% by volume in an isolating matrix, as compared with 30% for spherical materials.

It has been concluded that few, if any, materials are potentially useful as a conductive additive in the active mass of the positive electrode. The most promising materials are carbon fibres due to their good availability and cost, but these should preferably be coated with a doped tin oxide layer for oxidation protection. Such fibres have been shown to have a significant beneficial effect during formation of the plates. This is related to the decreased electrode potential and the increased conversion rate to lead dioxide. With these additives, however, a higher utilization of the positive active mass has only been found at low discharge rates and even then, the improvement is only modest, about 5%. At high rates of discharge, electrode capacity is not improved as acid diffusion becomes the limiting factor, not paste conductivity. When acid starvation is overcome, for example by use of the Eloflux technique, an increase in capacity of about 15% can be obtained, as is shown in Fig. 2.

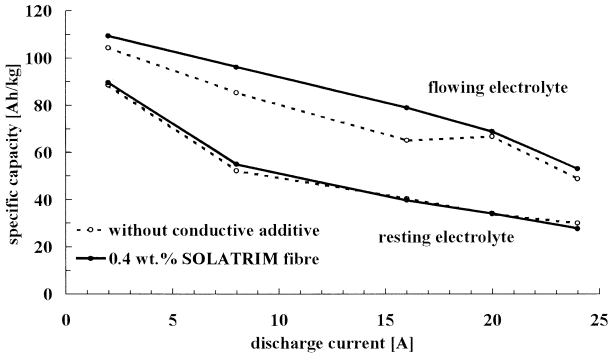

Fig. 2. Capacity of 10 Ah Eloflux Electrodes at different discharge rates.

It is also well known that carbon fibres are not stable in the positive plate under the onerous conditions encountered in lead acid batteries. Some 20% of the carbon fibre additive is lost during formation and it has been demonstrated that, on average, a further 1.5% is lost for each cycle. While attempts to protect the fibres with a tin oxide coating give some improvement, the coating was not sufficiently coherent to be adequate for practical application. It is thus concluded that, even if a stable conductive additive could be identified, it would only be effective in combination with other additives that are capable of acting either as an acid storage reservoir or a stimulant to acid movement.

Task 2. Electro-osmotic capacity enhancement [3].

As has been stated above, the discharge performance of positive plates in lead acid batteries is limited, particularly at higher rates of discharge, by diffusion of sulfuric acid electrolyte. Active material utilization and cell capacity may be enhanced by circulation of the electrolyte through the porous electrode. The concept of electro-osmotic irrigation of the positive active material was developed at AEA Technology on the basis of experience of the application of electro-osmosis to the removal of water from sludges, as well as on the observation of a large increase in the performance of chemical lead dioxide electrodes when using a binder with a large, negative zeta potential.

The objective of this Task is to select effective flow promoters, and to establish methods for incorporating them in lead acid cells in order to improve the availability of sulfate ions within the discharging positive plate. Lead sulfate, which is produced during the discharge of the cell, has a positive zeta potential which would induce an electro-osmotic flow out of the discharging positive plate. If a material of high negative zeta potential could be incorporated into one face of a positive plate, inward flow from that face, complementing ejection from the other face, may be expected to induce flow of electrolyte through the plate. Positive plates have been asymmetrically treated with materials that have high negative zeta potentials, such as

sulfonated polyvinylidene difluoride (SPVDF) and Nafion. Techniques include solution painting, solution spraying, and asymmetric pasting. In the last mentioned case, normal paste is supplied to one face and paste including electro-osmotic additive powders or coated fibres is applied to the other surface.

Unfortunately, discharge testing of treated plates has proved disappointing. Brush applications of SPVDF and Nafion solution yielded no performance advantage for treated plates. Indeed, in some cases, the treated plate surface was rendered hydrophobic and discharge capacity was reduced by up to 30%. Isolated enhancements of performance may be taken to indicate that deposition conditions may be highly critical and that performance of effective treatments may be destroyed by operation in the cell. Because of these problems, the anticipated test programme has been delayed.

As an alternative to the asymmetric application of the electro-osmotic promoter to the active material of the electrode, flow may be induced by an active membrane in contact with one surface of the plate. Significant flow of dilute electrolyte has been demonstrated for sulfonated porous PVDF membraness and for SPVDF and Nafion solution treated porous membranes. The flow measurements using battery concentration electrolyte require correction for both hydrostatic flow and ionic transport. Corrected acid transfers, equivalent to enhancements (relative to battery separators) of 10% of the discharge reaction requirement, have been measured for some of the treated membranes. In a new approach, low cost, battery compatible, porous membranes will be rendered hydrophilic and then surface fluorinated. Evaluation will initially be performed via dip-cell flow measurements. If success is achieved, single plate and cell testing will follow.

Task 3: On-board fast charging with Wavedriver power coupler [4].

The realization that both functions of motor drive and high-rate charging require the same power conversion circuitry, allows the same device to be put to dual use; this reduces the system cost significantly. A second major advantage of the combined drive-charger system is the low inherent cost of the off-board charging infrastructure required. This is because the power conversion and control electronics associated with the charging processes are, in this case, carried on-board the vehicle. The off-board requirements for a combined drive and charger reduces to a protected ac outlet, designed to supply power at a convenient rate. Single or multiphase supplies can be used, increasing application flexibility. Moreover, the operation of the power conversion equipment as a combined drive and charging system has further benefits.

The charging function requires a high degree of computational power. As a charger, the major function of the device, is to control precisely the energy flow into and out of the battery. In this mode, the charger monitors the terminal conditions of the battery. This function can be expanded at low cost to carry out all the duties of a battery-management system that include a varied range of charging algorithms. Charging algorithms can be refined for a particular manufacturer's battery. This process is carried out on a vehicle simulation rig.

Vehicle management can also be incorporated in the combined drive and charger. This 'systems approach' reduces the cost of the components of an EV and their installation effort—a key requirement for the EV as a mature product. The major elements of a combined drive and charger are shown in Fig. 3. The provision for a simple change-over switch allows the device to alternate between functions by connecting the three-phase output of the power conversion device to either the motor (drive function) or to the utility (charge function).

The experimental work in this programme was carried out utilizing a 312 V (26×12 V) string of Hawker 'Genesis' batteries and involved the testing of three different charging regimes on the combined driver-charger system with a PC interface—this is used for control and data

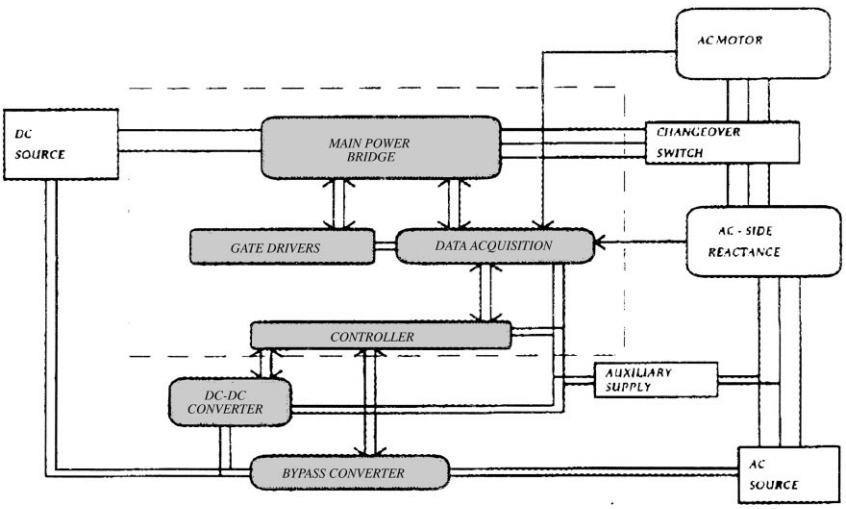

Fig. 3. Functional blocks of a Wavedriver combined drive-charger.

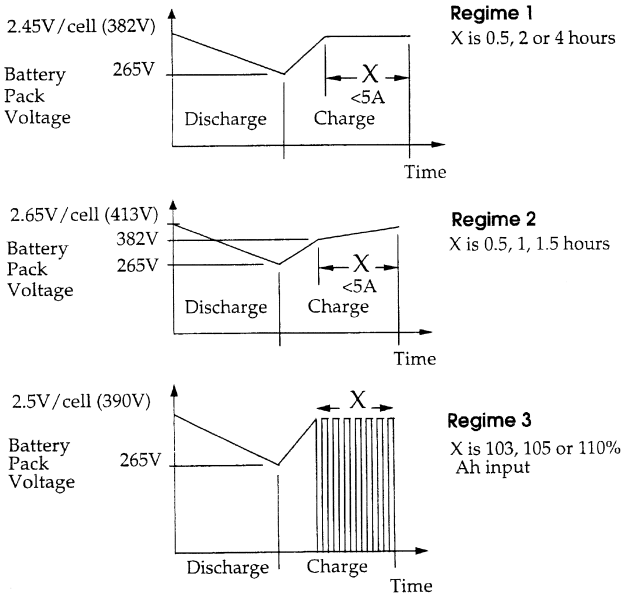

Fig. 4. Charging regimes 1, 2 and 3.

logging. The regimes are illustrated in Fig. 4 and are as follows.

Regime 1: Constant-voltage charging (382 V) until current falls to 5 A; continue charging for: (i) 0.5 h; (ii) 2 h; (iii) 4 h. Ten cycles of this profile are performed with a temperature compensation of 3 mV/cell/°C.

Regime 2: Constant-voltage charging (382 V) until current falls to 5 A; continue charging at 413 V for: (i) 0.5 h; (ii) 1 h; (iii) 1.5 h. Ten cycles of this profile are performed with a temperature compensation of 3 mV/cell/°C.

Regime 3: Maximum current charge until voltage reaches 390 V then 1 s, 390 V pulses followed by 1 s rests. Rest periods to be increased to ensure temperature does not exceed 45°C. Repeat for 103, 105 and 110% input. Ten charge–discharge cycles performed for each condition.

The results of this limited programme have demonstrated the feasibility of the proposed system. The two-step charge regime (regime 2) returned more capacity in less time than regime 1. In regime 2, the 0.5 h charge method is capable of returning sufficient charge to the battery in order that it can still deliver the normal 21 Ah (1 h rate) capacity. Also, the average charge time of the pulse-charge method (regime 3, 110% capacity returned) is less than that of the normal, single potential, charge method (regime 1, 0.5 h extra charge time). With the limited funding available, it was not possible to investigate other parameters such as higher power levels and shorter pulses.

Task 4: Improvement of cycle life [5].

Several factors may limit the cycle life of lead acid batteries, but one of the most complex degradation processes is related to changes in the positive active material. On cycling, the porous lead dioxide structure is modified and this modification is influenced to a great extent by the cycling regime, i.e., by the conditions of recharge and discharge of the battery. Therefore, battery performance is affected by the previous operating conditions. This 'memory effect' can be influenced by additives to the electrolyte, such as phosphoric acid, and can also be given a 'reset' by electrical treatment of the battery.

Investigations were performed with 160 Ah gel monoblocks and single cells of the same design. A comparison was made of the performance of batteries with and without phosphoric acid additions to the electrolyte. When no phosphoric acid is used, the capacity level is 5–10% lower with a 10 h initial recharge current than with a 4 h rate, both with full cycling (to 100% discharge) and also with partial cycling. With cells containing phosphoric acid, this effect is almost negligible, as the presence of the acid acts in a similar way to the beneficial effect of higher recharge rates; it changes the PbO_2 structure and assists both the recharge and the discharge reaction of the PbO_2 electrode. Designs containing phosphoric acid are superior when recharge is usually performed with a low-rate charger. In addition, simple constant-voltage recharge is possible.

Cycling in electrolyte containing phosphoric acid results in a finer PbO_2 pore structure with smaller average pore diameter, and an increased internal pore surface (BET) of the electrode. The porous PbO_2 structure is composed of smaller PbO_2 crystals after cycling in this type of electrolyte. This helps to explain why lower initial recharge current density is acceptable when phosphoric acid is present: a finer structure is created which, according to the 'agglomerate-of-spheres' model, is known to be beneficial for continuing cycling at high active material utilization. When phosphoric acid is not present, high initial recharge current density may act in a similar way; it enhances nucleation as distinct from crystal growth. As reported previously [1], the addition of phosphoric acid reduces the discharge rate dependency of the capacity significantly, giving a markedly lower capacity at low-rate discharges but a slightly higher capacity at very high rates (Fig. 5). This better high-rate performance can probably be explained by the higher internal surface of the cells containing the phosphoric acid.

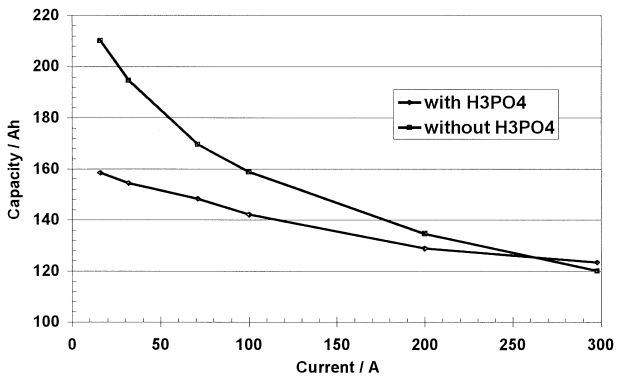

Fig. 5. Discharge capacity vs. discharge rate of cells with or without H_3PO_4 addition to the electrolyte.

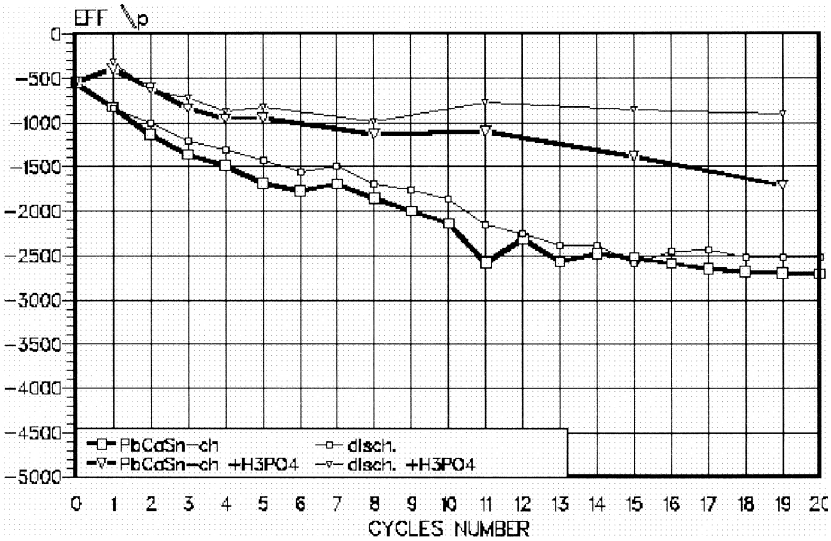

Fig. 6. Mechanical force exerted by PbO_2 active material: changes on cycling—discharged and recharged state.

During cycling, the apparent volume of the PbO_2 structure decreases during discharge and increases during recharge. This quasi-reversible behaviour can be monitored in situ by a special laboratory set up and may be related to the well-known successive volume increase during cycling which may promote active material shedding. Volume changes of the active material impose forces on its environment, i.e., on the grid, the separator, the negative electrodes and the cell container. When phosphoric acid is present in the electrolyte, a much more gradual increase of that force during cycling is observed, together with a much smaller difference between the forces exerted in the different states-of-charge (Fig. 6). When a dilatation force is exerted by a micro-screw on the PbO_2 material, much more ductile behaviour is found when phosphoric acid is present during cycling. These findings may help to explain the reduced tendency to softening and shedding of the PbO_2 structure, and the improved stability at a high capacity level with the phosphoric acid addition.

It has also been shown that it is possible to recover capacity in a battery by discharge at a very low rate. In the example given in Fig. 7, the battery was continuously operated for 620 cycles with discharge at 100 A and the capacity had dropped to below 100 Ah which was considered to be the end of life. At cycle 650, a low-rate discharge with 2 A to 1.8 V/cell was performed. Capacity on 100 A discharge increased by 27% from 95 to 121 Ah in the next cycle. When the cycling was continued, how-

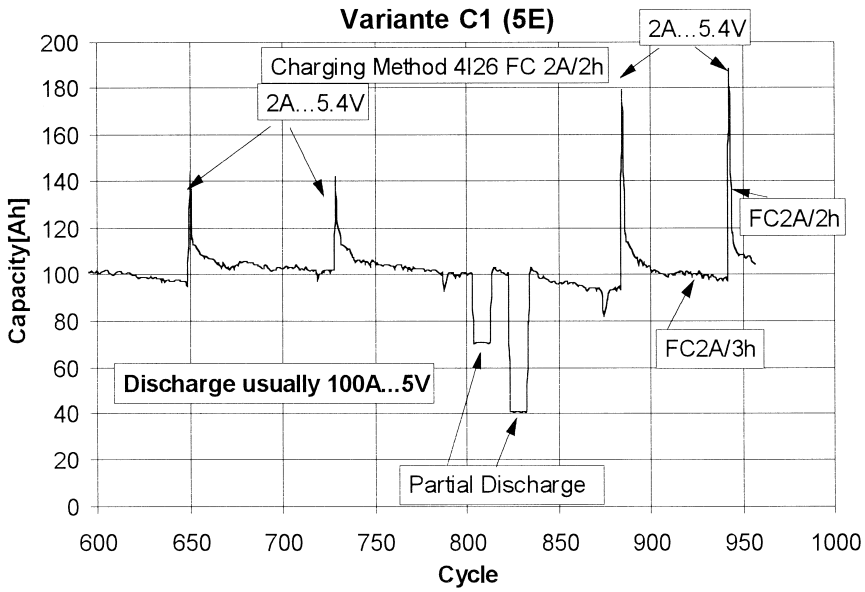

Fig. 7. Recovery treatment of positive electrode capacity lost on continuous cycling by low rate discharge applied four times.

ever, the capacity again decreased gradually but was above the 100 Ah limit for a further 75 cycles. At this point the low-rate discharge procedure was successfully repeated. Later, after an extended period with only partial discharge, the procedure was applied twice more. The increase in capacity was always about 25% or more and gave about 75 more cycles before the end-of-life capacity limit of 100 Ah was again reached. This is an interesting phenomenon, but whether it has a practical role in extending battery life is debatable.

Task 5: Influence of curing and formation on cycling at high rates [6].

In this Task, accelerated cycle testing was carried out on AGM cells with different types of flat positive plates. The plates were made with various paste densities and by using different curing and formation programmes. Paste densities of 4.3, 4.0 and 3.8 g/cm^3 were employed. For curing and drying, a laboratory curing chamber was used in which both temperature and humidity could be precisely controlled. The humidity was 95% during curing and 30% during drying; the drying temperature was 50°C. In order to obtain tribasic lead sulfate (3BS), tetrabasic lead sulfate (4BS) or a mixture of the two, three different temperatures were used during curing namely 50, 70 or 80°C. After drying, the plates were analyzed; the results are given in Table 2.

The influence of different soaking times (0.5, 2, 5 and 24 h) in acid of either 1.06 or 1.20 specific gravity was also investigated. Investigations of the plates after soaking showed that, in the case of plates cured at high temperature (4BS), the initial reaction is to monobasic lead sulfate, with a later gradual reaction to lead sulfate. With 3BS, there is a relatively fast reaction to lead sulfate. In both cases, the reaction proceeds more slowly in acid of lower specific gravity.

The plates were formed in tanks with sulfuric acid (325 ml per positive plate, 1.06 specific gravity) under three different formation programmes, namely:

(i) constant-current formation, $I = 1.5$ A for 43 h;

(ii) constant current, $I = 1.9$ A for 24 h, followed by a discharge step with 1.5 A for 4 h and a further charge step at 1.23 A for 24 h.

(iii) pulse formation for 43 h (10 s pulse $I = 3$ A with 10-s rest at zero current).

Table 3
Initial capacity of positive plates with different formation programmes

Formation type	Plate type	Initial capacity (C_5) Ah
(a) Constant current 1.5 A for 43 h	4BS—4.0 g/cm^3	7.8
	4BS—4.3 g/cm^3	7.5
	3BS—4.0 g/cm^3	13.5
	3BS—4.3 g/cm^3	13.6
(b) With discharge step	4BS—4.0 g/cm^3	13.0
	4BS—4.3 g/cm^3	12.9
	3BS—4.0 g/cm^3	15.0
	3BS—4.3 g/cm^3	14.2
(c) Pulse formation	4BS—4.0 g/cm^3	11.1
	4BS—4.3 g/cm^3	10.4
	3BS—4.0 g/cm^3	14.2
	3BS—4.3 g/cm^3	13.3

The total amount of charge was always 64 Ah. Table 3 shows how these different programmes affected the initial capacity of the various types of plate. It can be seen that formation with a discharge step, or a pulse formation technique, helps to overcome the inherently inferior formation capability of the high-temperature cured mass.

Following the characterization work on curing and formation, cycling tests were conducted. In the first series of tests, accelerated cycling of single positive plates was carried out with an excess of electrolyte and of negative mass. Six different types of plate were used, namely, paste densities of 4.3 and 4.0 g/cm^3 in combination with 3BS, 4BS, and a mix of 3BS and 4BS. The positive plates were placed between two counter negative plates with acid of specific gravity 1.30. The discharge current during cycling was 11 A down to 1.5 V, and the charge current was 2.8 A up to 2.4 V followed by an additional charge at 0.7 A for 6 h. These were arduous conditions and all plates failed within 70 cycles. The weight loss of the positive plates was determined in order to ascertain the amount of shed material. It was found (Fig. 8) that the influence of paste density and curing conditions on shedding agreed well

Table 2
Characteristics of cured plates

Paste density (g/cm^3)	Curing temperature	Crystal size	3BS (%)	4BS (%)	Pore diameter (μm)	BET (m^2/g)
3.8	high	large	0	81	11	0.3
4.0	high	large	3	81	9	0.4
4.3	high	large	0	81	6	0.4
3.8	low	small	50	0	0.6	1.2
4.0	low	small	52	0	0.5	1.3
4.3	low	small	41	0	0.4	1.2
3.8	medium	large/small	38	28	0.8	1.0
4.0	medium	large/small	28	33	0.7	0.9
4.3	medium	large/small	30	37	0.8	0.9

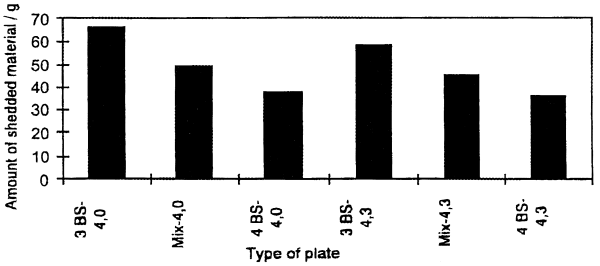

Fig. 8. Amount of positive material shed after an accelerated cycle test in a flooded system.

with the decrease in capacity observed during cycling; 4BS gave the best performance, i.e., the least shedding. This is valid for both paste densities but the amount of shed material was in general higher with the lower paste density.

The majority of the cycling tests were carried out on 2 V AGM cells with a nominal capacity of 24 Ah at the 5 h rate. These cells had three positive plates enveloped in glass mat separators (approximately 35% fine fibre and 25% compression) and four negative plates. Again a rigorous cycling regime was used with a discharge current of 34 A down to 1.5 V and a constant-current charge of 10 A up to 2.4 V with a charge time of 7 h. Fig. 9 shows the influence of paste density and curing on cycle life, and it can be seen that the behaviour in AGM cells is in contrast to that observed in the flooded design. The cycle life is much better with AGM and in fact the 3BS and 3BS/4BS mix behave much better than 4BS cured plates. There is also a marked influence of paste density, with the lower paste density giving a worse cycle life. Fig. 10 shows the effect of the formation process on cycle life which, in the case of 3BS, appears to have no influence. With 4BS plates, there does appear to be some influence, with pulse formation providing the poorest performance. The results do clearly show, however, the generally inferior behaviour of the 4BS cured plates.

It is also interesting to note that, as part of these experiments, some cells were produced and cycled with phosphoric acid addition. All failed in less than 200 cycles and thus it would appear that the influence of phosphoric acid in AGM cells is very different to that in gel batteries.

Task 6: Separator optimisation [7].

This task was designed to establish the influence of the percentage of fine fibre content and the percentage of compression of absorptive glass mat separators on the performance and life of the battery. In order to achieve this a 3×3 matrix experiment was designed as follows.

Three different types of separator	50% fine fibre
	66% fine fibre
	75% fine fibre
Three different compression levels	20% compression
	25% compression
	30% compression

The cells were built by Oldham France, based on a standard valve-regulated design, and initially subjected to stratification testing. The results have been reported previously [1] and can be summarized as follows:

- Fine fibre content above 66% has no further effect on stratification.
- Compression is important: 20% is too low, 25% is better, but there is no apparent improvement at 30%.

Life-cycle testing was carried out by Entek International according to the following regime:

- discharge: 3 h at $C_5/4$ (75% DoD)
- charge: 12 h at $C_5/5$ (limited to 2.35 V/cell)
- capacity check: At 10 cycles, 50 cycles, and then every 50 cycles three discharges at $C_5/5$ to a final voltage of 1.70 V/cell.
- failure point: C_5 capacity $< 75\%$ initial C_5 capacity after three capacity discharges.

The results of the life-cycle tests for the different fine-fibre types are illustrated in Figs. 11–13. The battery

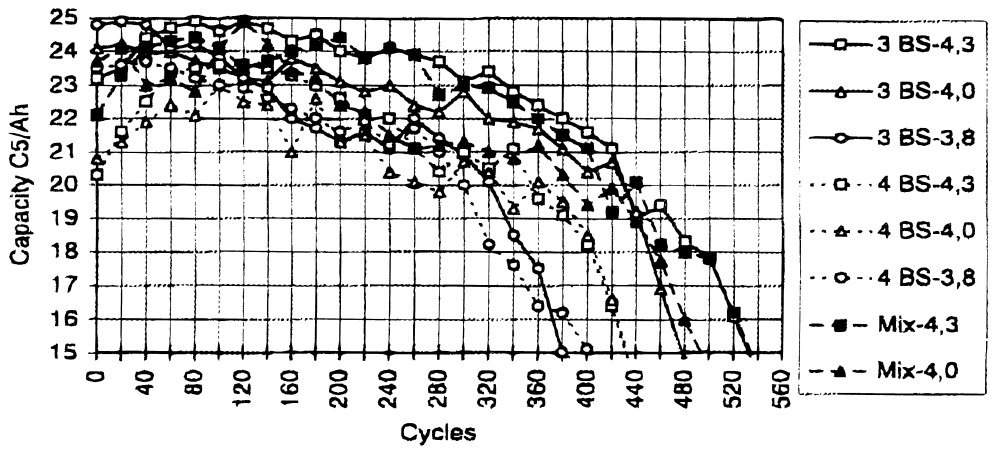

Fig. 9. Influence of paste density on cycle life in AGM cells (2 h soaking and constant current formation).

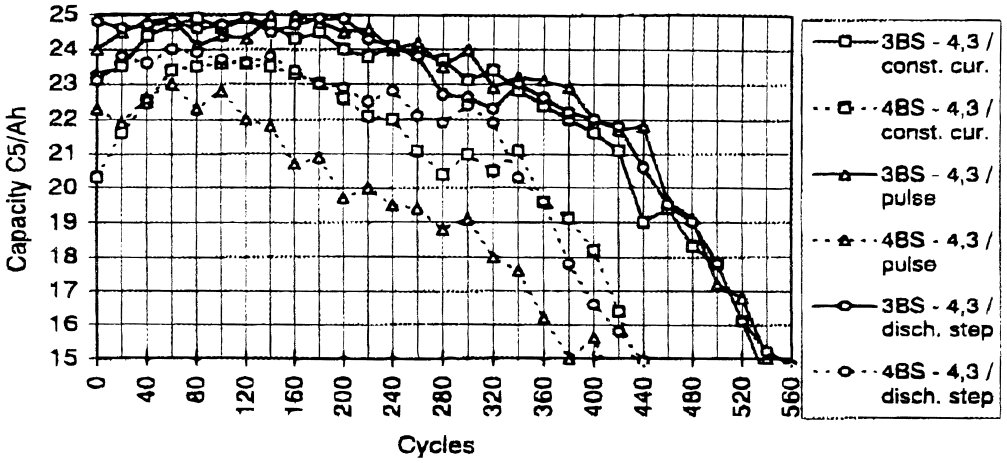

Fig. 10. Influence of curing method with different formation methods.

builds with the lowest fine-fibre content (50%) and 20 and 25% compression failed after 200 cycles. After 2 months on open circuit, however, the capacity of these batteries was checked again and was found to have recovered. They were put back on cycle testing and achieved a total of 400 cycles before failing again. In general, the influence of compression and fine-fibre content can be summarized as follows.

- 50% fine fibre: 20 and 25% compression—failure at 400 cycles; 30% compression—capacity fell to $<80\%$ at 100 cycles, recovered to $>80\%$, failed at 750 cycles.
- 66% fine fibre: 25% compression—failure at 500 cycles; 20 and 30% compression—failure at 900 cycles; from 200 cycles onwards, 20% had higher capacity than 30%.
- 75% fine fibre: 30% compression—failure at 825 cycles; up to 450 cycles, 30% compression retained the highest capacity but, at the end of life, the capacity was similar; 20% and 25% compression cells still cycling just above 75% of original capacity when the tests were terminated at 900 cycles.

Initially, the batteries with high compression/high fine-fibre content performed the best with the lowest initial loss of capacity, although by the end of cycle testing the results were less clear cut. It is possible that by the end of the test there is some degradation of the fine fibres in the higher fine-fibre content separators and this results in a loss of compression. The fact that, at 66% fine fibre, the 20% compression cells behaved better than the cells at higher compressions is not so easy to explain. Tear-down analysis of all the cells is now in progress.

Task 7. Influence of DoD as a function of discharge rate on battery life [8].

The DoD is thought to influence the life of lead acid batteries in such a way that, by increasing the DoD, the life of the battery is reduced. In practice, therefore, it is assumed that it is important to prevent the batteries from deep discharging to protect their life. The influence of DoD can become less important at higher discharge rates because of lower available capacity and thus a higher DoD may be allowable with increasing discharge rate.

The tests were carried out on 6 V Dryfit traction gel batteries (3TZ AX7) batteries, manufactured by Sonnen-

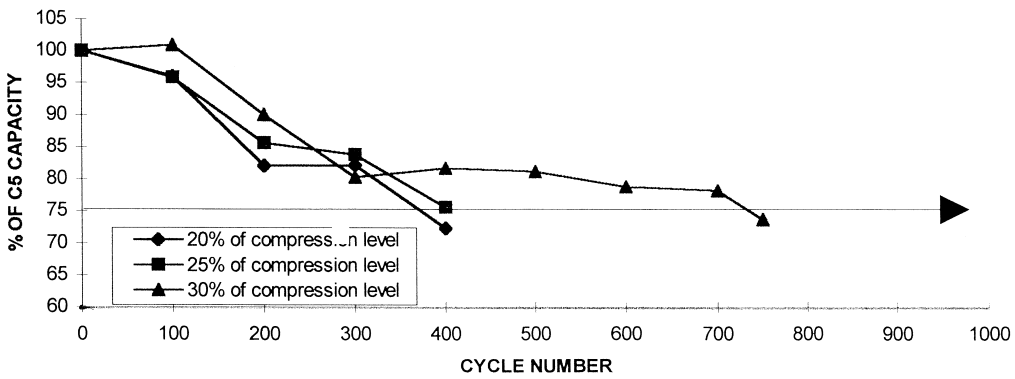

Fig. 11. Discharge capacity development (50% fine fibre) at different compressions.

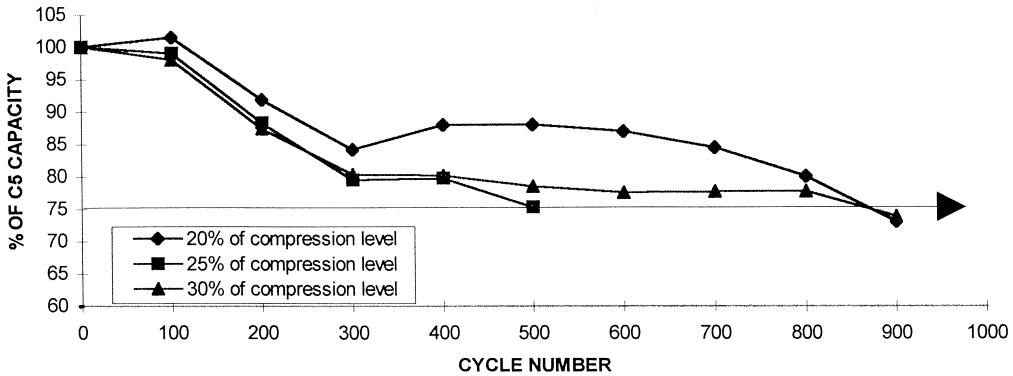

Fig. 12. Discharge capacity development (66% fine fibre) at different compressions.

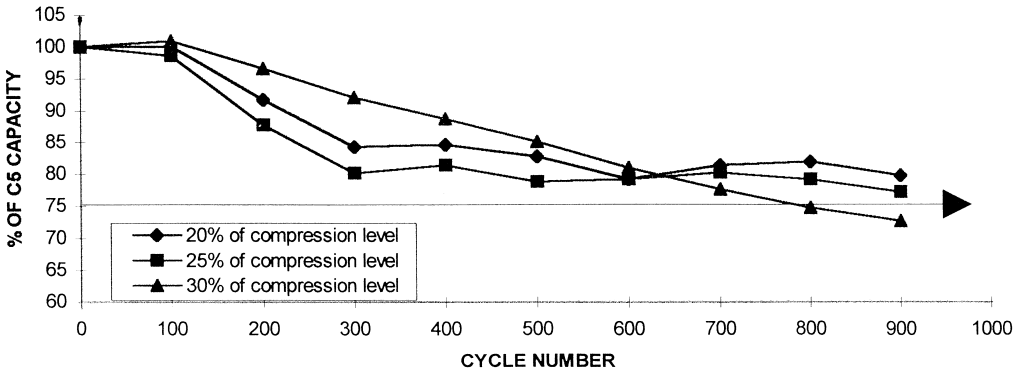

Fig. 13. Discharge capacity development (75% fine fibre) at different compressions.

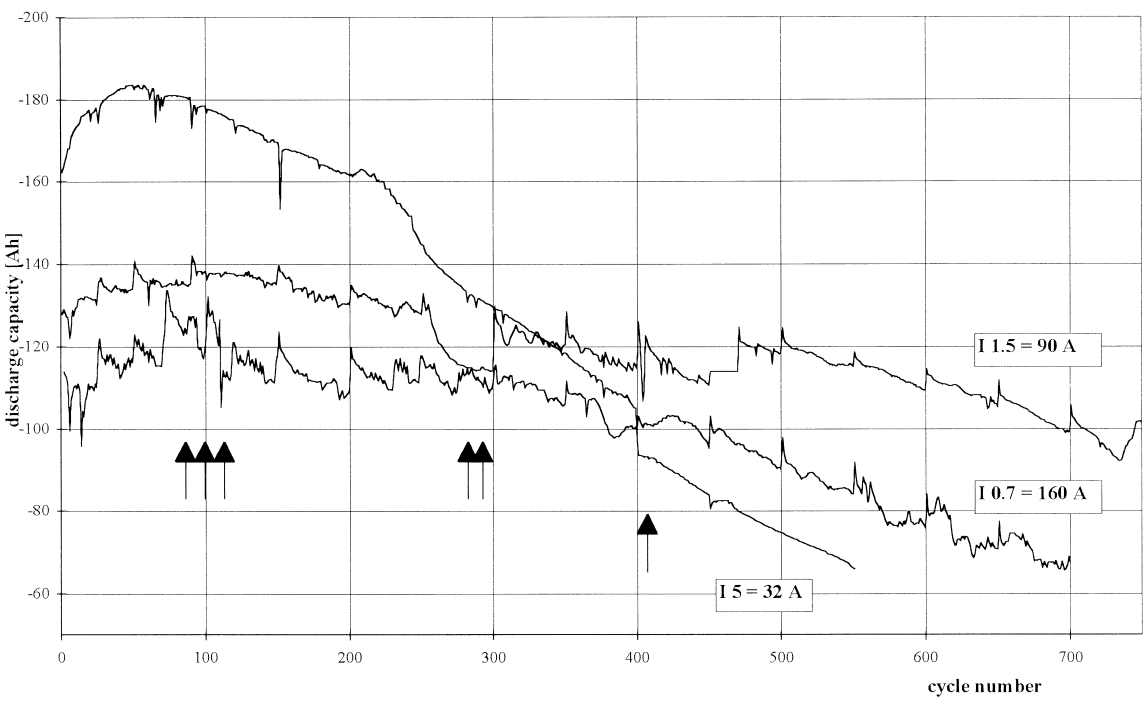

Fig. 14. Development of capacity for batteries discharged to 100% DoD at different discharge rates.

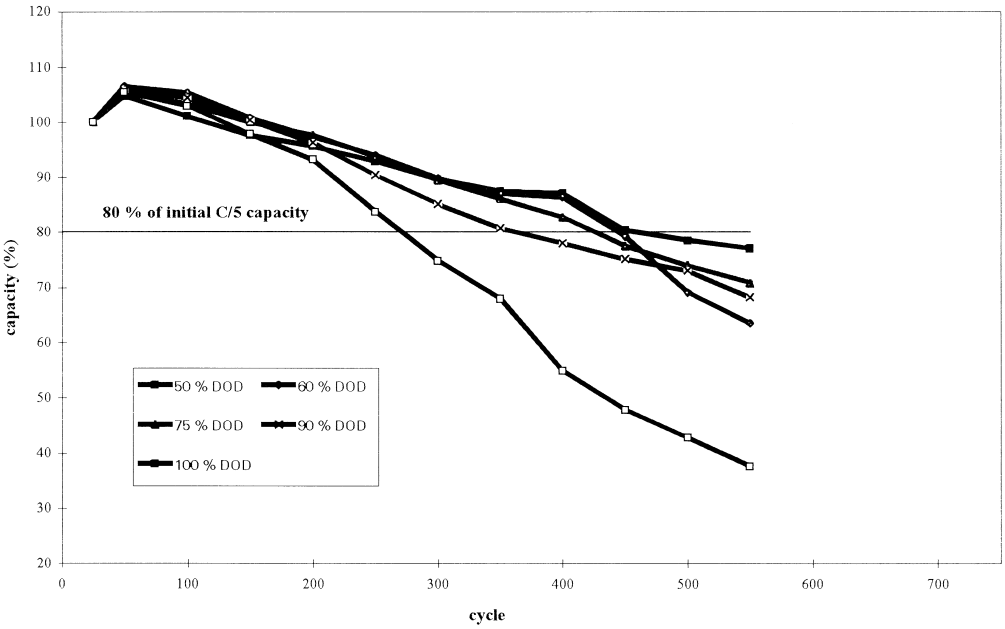

Fig. 15. Development of normalised C_5 capacity for batteries cycled at $C_{5/5}$ discharge rate to different DoDs.

schein, with a nominal capacity at the C_5 rate of 160 Ah. Three different discharge rates were employed, namely, $C_{0.7}$, $C_{1.5}$ and C_5 with discharge starting 1 h after the last battery at each discharge rate has finished the charge phase. The batteries were discharged to different DoDs (100, 90, 75, 60 and 50%) corresponding to each discharge rate or until the voltage falls below 1.7, 1.65 or 1.5 V/cell for the C_5, $C_{1.5}$ and $C_{0.7}$ discharge rates, respectively. Charging was carried out using an IU characteristic, the charging started 0.5 h after the last battery for the given discharge rate finished the discharge. The charge current was 32 A (I_5) for all batteries, independent of the discharge rate and the DoD. When a voltage of 7.2 V is reached, charging continued, either until the current fell

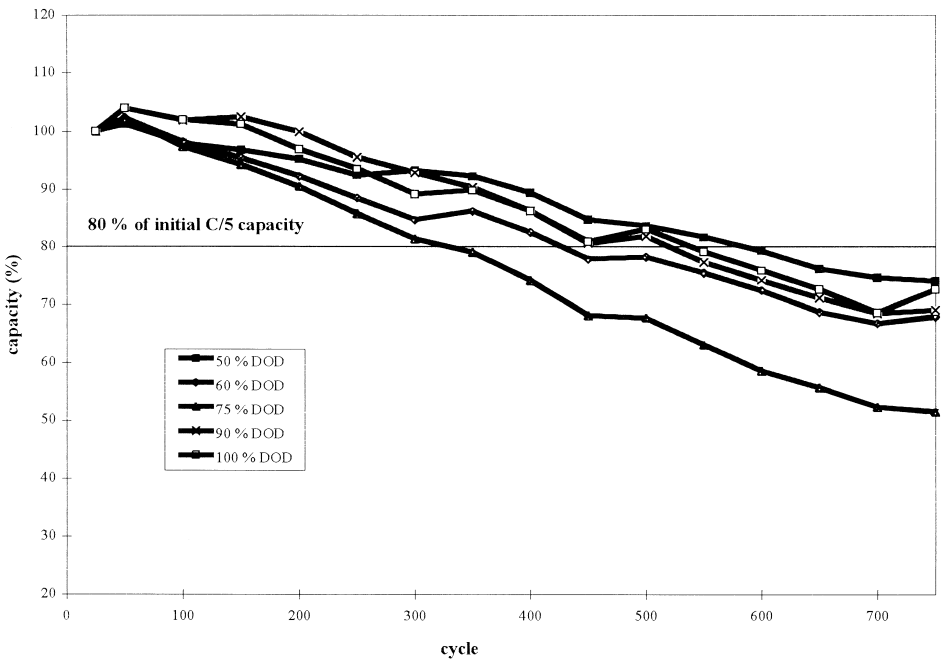

Fig. 16. Development of normalised C_5 capacity for batteries cycled at $C_{1.5}$ discharge rate to different DoDs.

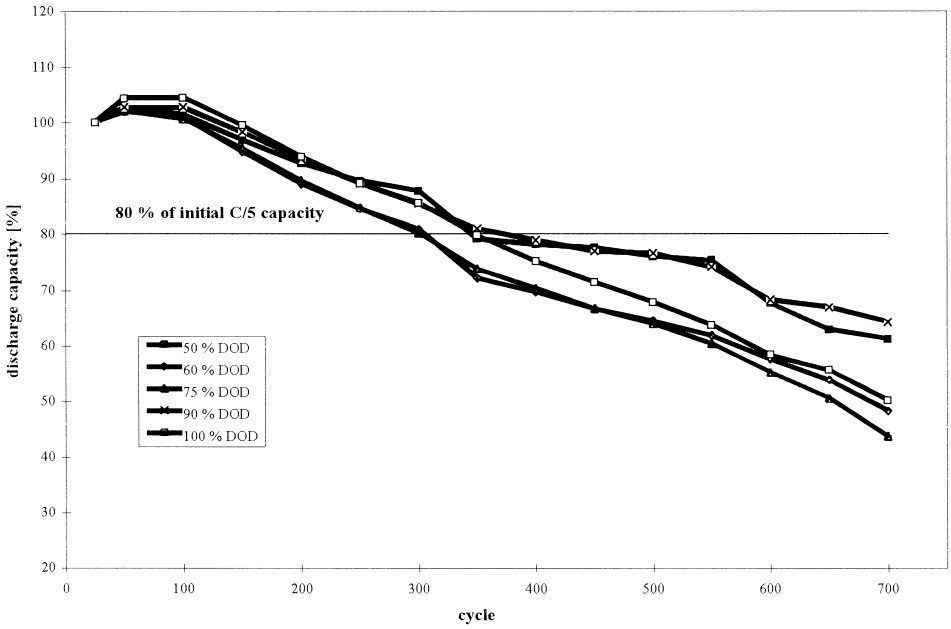

Fig. 17. Development of normalised C_5 capacity for batteries cycled at $C_{0.7}$ discharge rate to different DoDs.

below 320 mA for each individual battery or until a time limit of 15 h was reached. Capacity checks were carried out every 50 cycles and the test was concluded if the capacity fell below 80% of the nominal C_5 capacity. Three batteries were used for each combination of discharge rate/DoD.

Fig. 14 shows the development of the average capacities for the batteries discharged to 100% DoD at the three different discharge rates. In general, it can be seen that under these conditions the decrease in capacity is the fastest at the $C_5/5$ discharge rate; this is related to the higher utilization of the active mass. At the $C_{0.7}$ discharge

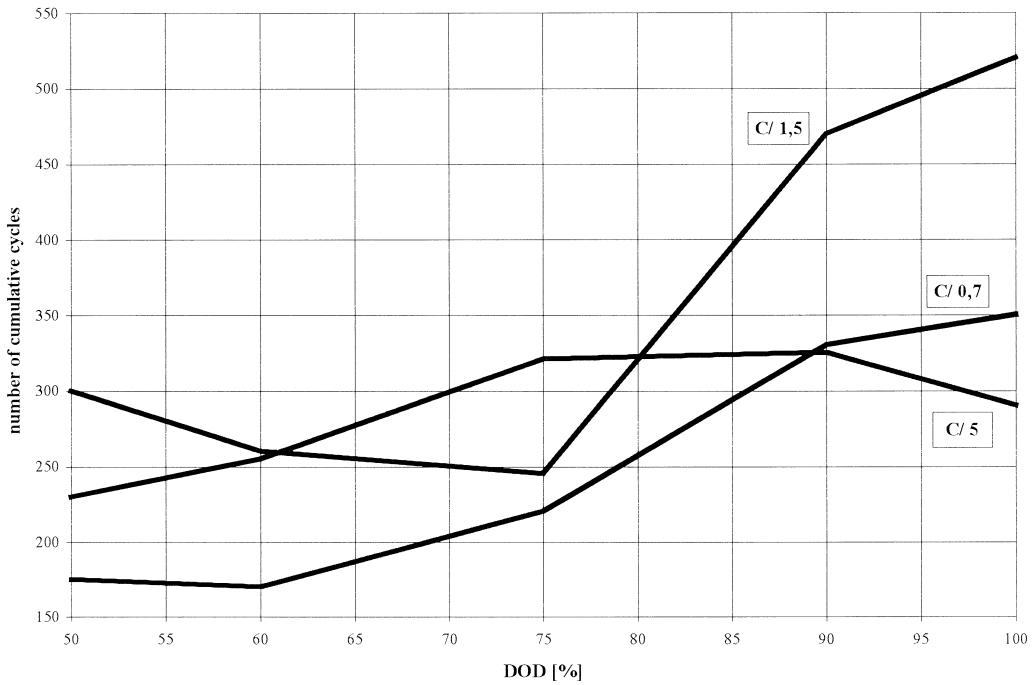

Fig. 18. Number of full cycles to less than 80% capacity for different DoDs and discharge rates.

Table 4
Vickers hardness of gravity-cast grids at different stages of testing

Alloy	As-cast	72 h at 60°C	340 h at 60°C	3 months at 20°C	After curing and formation
Reference	15.0	16.8	16.0	16.8	16.1
Sn-rich	16.3	21.6	18.3	19.5	19.0
Ag-rich I	15.8	19.3	17.6	18.3	16.8
Ag-rich II	17.9	18.6	18.1	20.0	18.3

rate, the utilization of the active mass is lowest but the decrease in the capacity after about 300 cycles is faster than for the $C_{1.5}$ discharge rate. That would suggest that, besides the different utilization of the active mass, there is a second effect of the discharge rate on the cycle life. At very high discharge rates, the ageing of the battery is faster even when the utilization of the active mass is lower.

The development of the C_5 capacity vs. the cycle number for the different cycling rates and the different DoDs is summarized in Figs. 15–17. The capacity of each individual battery has been normalized to the individual capacity at cycle number 25 and each point drawn represents the average value of three batteries. For cycling at the $C_5/5$ discharge rate (Fig. 15), the capacity of the batteries discharged to 100% DoD on every cycle falls faster followed initially by the decrease in capacity for the batteries discharged to 90% DoD. No significant difference in the development of capacity for batteries discharged between 50 and 75% DoD could be observed. For cycling at the $C_{1.5}$ and $C_{0.7}$ rates (Figs. 16 and 17), the development of the capacity is less sensitive to the discharge rate but, in both cases, the fastest decrease in capacity is observed at DoDs of 60 and 75%. It is interesting to compare the total amount of energy stored in the battery during cycle life as influenced by the discharge rate and DoD. The number of full cycles completed before the capacity drops below the 80% nominal capacity value is related to the total driving range of the battery during its life and is therefore important. The number of full cycles vs. DoD for the different discharge rates are presented in Fig. 18. The data suggest that at high rates of discharge, greater DoDs produce more total energy during the life of a battery or, possibly, that partial discharges, followed by recharge may be detrimental. It should be noted that these results have been obtained with gel batteries under conditions of constant-current discharge at room temperature. With different battery types and under dynamic driving cycling usage results could be different.

Task 8: Effect of alloying elements on grid properties [9].

A way to improve the specific energy of a lead acid battery is to reduce the grid weight relative to the active material. As far as the positive grid is concerned, this means the development of stronger and more corrosion-resistant alloys. The work in this task has shown that tin or silver additions to conventional lead–calcium–tin alloys used in automotive batteries can improve the grid material in terms of:

- highly improved mechanical properties (creep resistance)
- higher corrosion resistance
- better charge transfer between the grid and active mass.

The alloys selected for evaluation (Table 4) were chosen on the basis of earlier work and then subjected to industrial evaluation. Since the actual material that starts battery life in service experiences thermal treatment during the curing and formation steps of plate production, all samples were held at 60°C for 72 h. During this process, it was observed that age-hardening is speeded up dramatically. As age-hardening materials can also soften in time through overageing, long-term tests at 60°C were also performed. Alloy hardness values after casting and treatment are shown in Table 5. The simulation of the curing and formation steps seems to be validated by the data in the second and fifth columns. It confirms the gain due to thermal treatment during the plate-preparation process.

Table 5
Initial parameters of the 192 V, 50 Ah batteries (variants N and S)

Parameter		Capacity (Ah)		Average Power (W/kg)		Specific Energy (Wh/kg)	
Rate	Current	Type N	Type S	Type N	Type S	Type N	Type S
C1	**50**	33.2	35.9	34.9	34.2	22.7	24.7
P1	**33**	36.0	38.2	23.0	24.7	24.8	25.9
C2	**25**	41.0	43.7	17.4	17.5	28.3	30.2
C5	**10**	51.0	53.0	7.1	7.3	35.3	36.6
ECE-15		37.8	39.6	14.4	15.0	22.6	24.5
ECE-15L		42.3	42.6	10.0	10.2	26.3	26.7

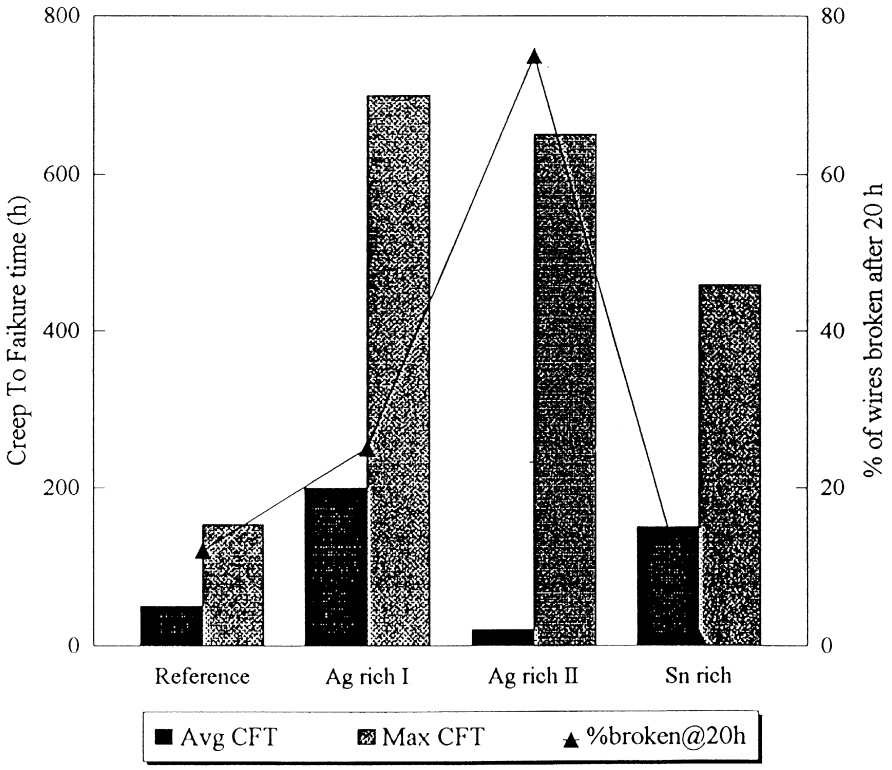

Fig. 19. Creep resistance of grid wires.

Fig. 19 shows the effect of tin and silver on the creep resistance at 27.2 MPa, for wires from industrially-cast grids. The creep resistance is represented by failure times (average and maximum) and by the percentage of grid wires broken after 20 h. The data indicate a sensitivity to failure due to surface defects and intrinsic brittleness of the material. This demonstrates that tin and low silver additions increase, by a factor of three, the creep resistance of the reference alloy. It also shows that a high silver content renders the alloy too brittle (almost 80% of the wires are broken after 20 h). This brittleness also showed up during pasting of the plates.

Corrosion tests have shown that both tin and silver improve corrosion resistance significantly, although there is only a marginally additional improved performance when these two elements are used together. Tin, at a content of over 1 wt.%, also improves the conductivity of the corrosion layer.

For battery trials, accelerated TC69 cycling tests were carried out on two 12 V, 55 Ah batteries for each alloy candidate, with gel electrolyte but without phosphoric acid addition. Fig. 20 clearly indicates that the batteries using the tin-rich and silver-rich I alloys retain the highest capacity and longest cycle under 100% DoD cycling in this test. There seems to be a true alloy effect even if, on dismantling the batteries, the failure mode was not due to excessive grid corrosion, but probably linked to a softening of the positive active mass. Because of the rather low cycle life (the design of these batteries was not optimized), no distinction can be drawn between the alloys in terms of

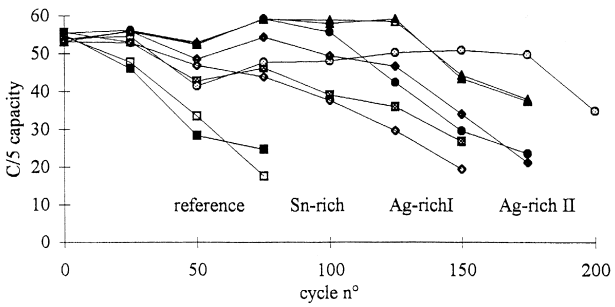

Fig. 20. TC69 cycling test—C_5 Capacity vs. number of cycles.

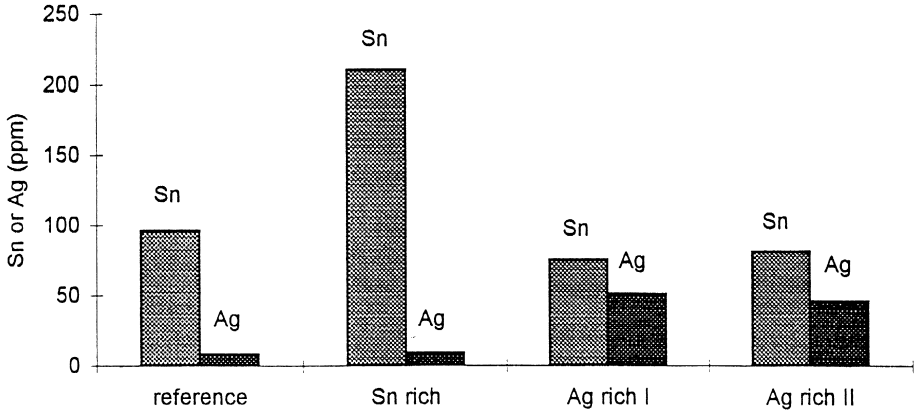

Fig. 21. Analysis of negative active material after cycling.

grid growth (< 0.4%), water loss (60 g) and grid weight loss (5% per 100 cycles). Nevertheless, analysis of the positive and negative active-masses reveals that positive-grid corrosion releases tin or silver into the battery and that these migrate to the negative plate. Results are given in Fig. 21. As the electrochemical behaviour of tin is very similar to that of lead, it is not thought that this will harm the negative plate. Silver, however, with its ability to promote hydrogen evolution could be a problem, and it may also affect self-discharge behaviour. Tests are in progress to evaluate this.

Thus, although both the tin-rich and silver-rich I alloy have been shown to have benefits, the fact that the silver alloy is:

- more expensive
- may impact on gassing at end of charge
- adversely affect self discharge
- present some recycling difficulties

resulted in a preference for the tin-rich alloy as the alloy to be used in Task 9.

Task 9: Manufacture and testing of prototype batteries [10].

The initial work programme for the Project envisaged the construction in Task 9 of up to six variant battery designs for parameter testing and three for full life-cycle testing under the Eucar ECE-15 test procedures. During the course of the work on the previously described tasks, an advisory team was set up to consider the variants to be built. This was convened at the end of the second year as it had become clear that the testing would take longer than the 12 months initially allowed. Thus, battery designs had to be formulated so that construction could begin in July 1996 and testing commenced in October of that year. Therefore, was not possible to have access to the full programme results by the time decisions on certain battery parameters had to be taken. Also, it was not feasible to do parameter testing on the six variants and then select the batteries for life-cycle testing in view of the time limitations. Even with parameter and life-cycle testing running concurrently, testing would run beyond the end of 1997 for 500 cycles.

As the additive work had not been successful in achieving increased specific energy, it was decided that the programme would be orientated towards evaluation of the alloy work but with an emphasis on good cycle life. Thus, following discussions within the Advisory Committee, it was agreed that the following designs should be built for parameter testing:

- a standard design optimized for life, with an AGM separator (N);
- a standard design optimized for life with a gel construction (G);

Table 6
Initial parameters of the 192 V, 50 Ah batteries (variants N and S)

Parameter		Capacity (Ah)		Average Power (W/kg)		Specific Energy (Wh/kg)	
Rate	Current	Type N	Type S	Type N	Type S	Type N	Type S
C1	**50**	33.2	35.9	34.9	34.2	22.7	24.7
P1	**33**	36.0	38.2	23.0	24.7	24.8	25.9
C2	**25**	41.0	43.7	17.4	17.5	28.3	30.2
C5	**10**	51.0	53.0	7.1	7.3	35.3	36.6
ECE-15		37.8	39.6	14.4	15.0	22.6	24.5
ECE-15L		42.3	42.6	10.0	10.2	26.3	26.7

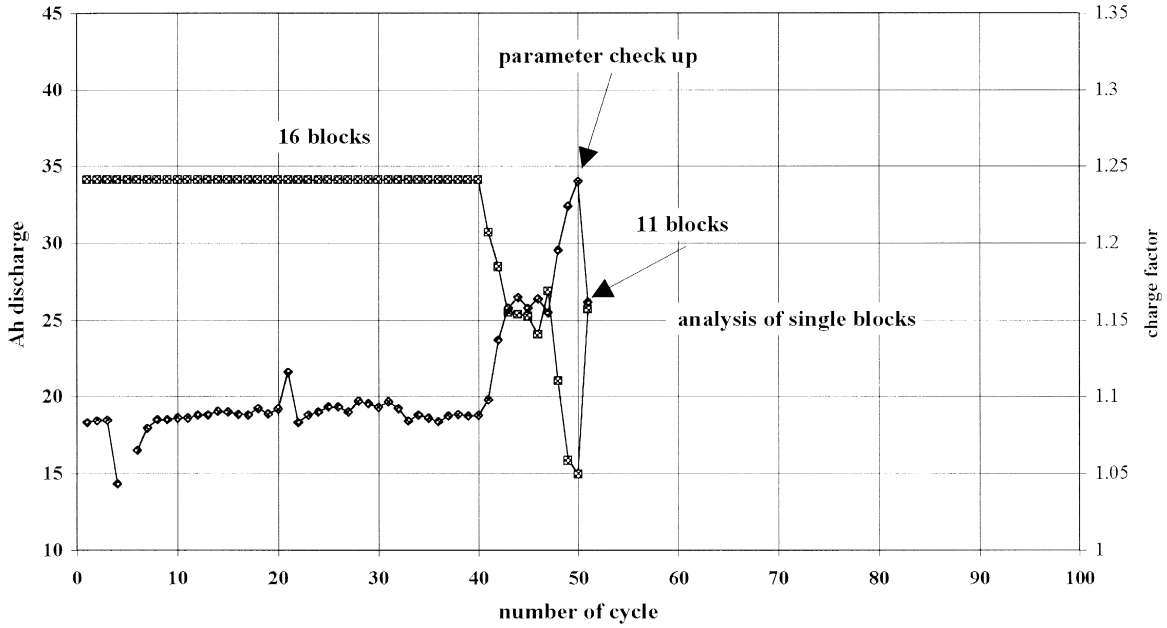

Fig. 22. Development of discharge capacity and charge factor during cycling of Type S battery.

- a standard design with low density paste for increased specific energy (S);
- a novel 'strap tubular' design based on ALABC work at the Central Laboratory for Electrochemical Power Sources in Bulgaria (P).

These would all be built into a standard FIAMM case and would use positive grids cast from alloy developed in Task 8 (except for Type P). For the standard design, the thickness of the positive plates was 1.75 mm (154.2 g) and that of the negatives (Pb–Ca alloy) was 1.05 mm (99.5 g).

For cycle-life testing, the standard design options would be considered plus the Type N design cycled in conjunction with the T-Cheq charge equalizer developed in the ALABC programme RMC-004A (designated Type C). As it turned out, because of the space limitations imposed by the FIAMM case and the other components, Varta found it

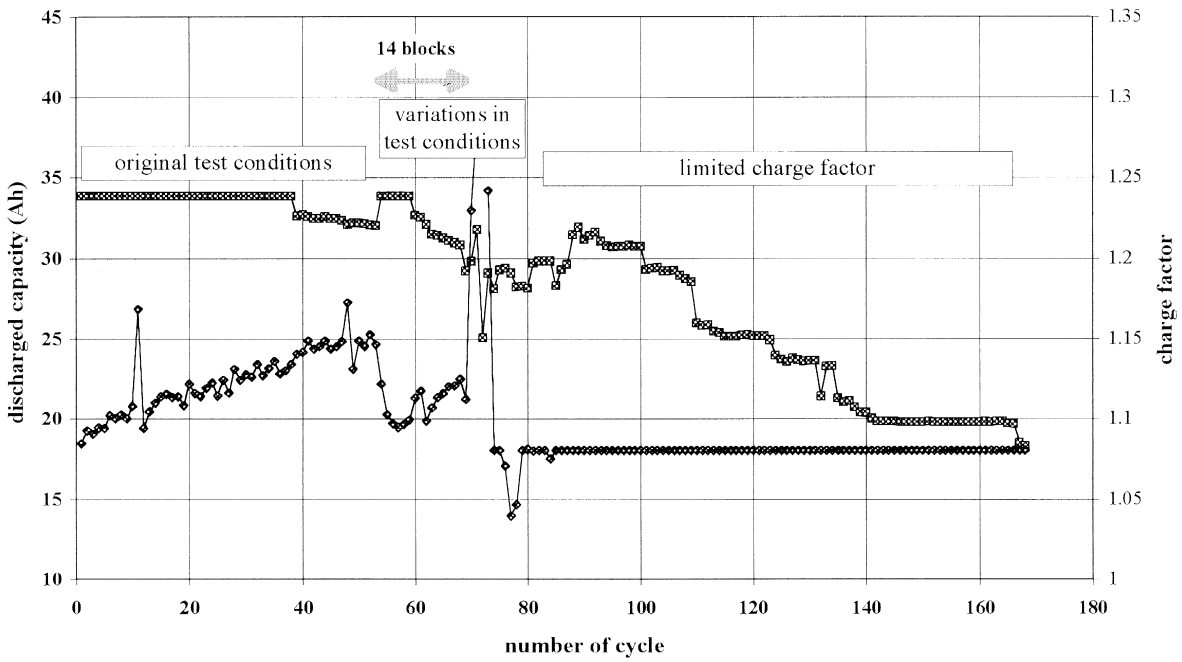

Fig. 23. Development of discharge capacity and charge factor during cycling of Type N battery.

impossible to fill the gel batteries and work on this option was suspended. Parameter testing of the remaining variants (as a 192 V battery) started in October and were remarkably close to the design predictions with specific energies of 35 and 37 Wh/kg for the standard and higher specific energy designs, respectively. The full parameter test results are given in Table 6 and demonstrate the slightly improved performance of the higher specific energy variant. The effect of the charge equalizer was to improve the performance of the standard Type N batteries closer to that of the Type S variant.

Life cycling was carried out using the ECE-15L 80% cycle. Initial performance of the three batteries was evaluated under the ECE-15L dynamic discharge test (an average of three tests) and the 80% value determined. These were found to be as follows.

Type N	capacity = 42.3 Ah	80% value = 33.8 Ah
Type C	capacity = 39.2 Ah	80% value = 31.4 Ah
Type S	capacity = 42.6 Ah	80% value = 34.1 Ah

Using the 80% value for each string, the cycle is terminated when this amount has been discharged or when the voltage of one individual block in the string falls below a defined cut-off voltage. The development of the capacity and of the charge factor for the batteries are shown in Figs. 22–24. For all three strings, it can be observed that the decrease in capacity is accompanied by an increase in the charge factor, and the very high charge factor seems to accelerate the loss in capacity. For all three strings, the capacity drops below the 80% value of the initial ECE-15L capacity around cycle number 40 (discounting the 35 + cycles used in the parameter testing). For string S (Fig. 22) the capacity loss is very dramatic. For string N (Fig. 23), the capacity was returned to above 80% by removing two blocks but only for a few cycles. Even when the charge factor was controlled (from cycle 80) the capacity decreased continuously to an unsatisfactory level after a short period of recovery. As can be seen from Fig. 24, even the use of the charge equalizer does not stop the decrease in capacity at 40 cycles and the gradual increase in the charge factor. At that time, the charge equalizer showed that high equalizing currents were flowing between the different blocks; this indicated that the remaining capacity of the individual blocks in the string already differed significantly. In this case, the charge factor was controlled from cycle number 90 and, after several cycles with the capacity around 25 Ah, it suddenly increased before starting to decline again. No explanation has been found for this as there was no interruption in time, no change in temperature, and no alteration of the charge regime. Discounting the first capacity decline, the battery achieved some 135 cycles prior to dropping below the 80% level; perhaps this indicated some benefits of the charge equalizer.

The above performance obviously represents a most disappointing outcome for the demonstration phase of the Project and intensive work is underway to determine the cause(s) of the failure. Tear-down analysis has been carried out and the following observations have been made.

- the positive active mass is very soft;
- there is bad adhesion of the positive active mass to the grid;
- on removing the separator, a large amount of the positive paste remains attached to it;

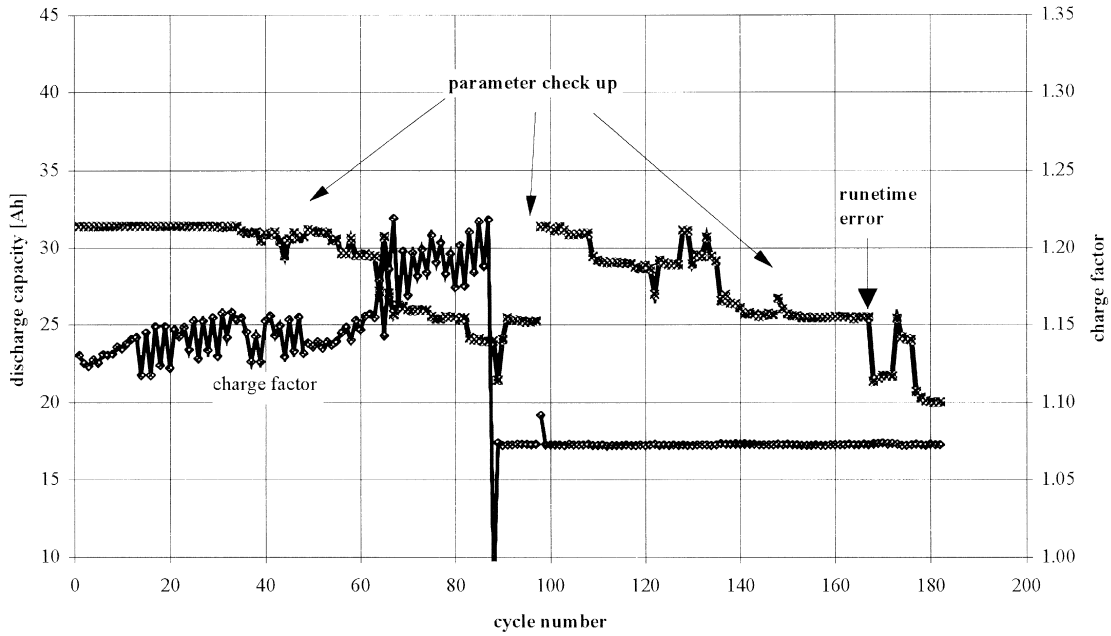

Fig. 24. Development of discharge capacity and charge factor during cycling of Type C battery.

- there are no problems with corrosion of the positive grid;
- the negative plates remain in very good condition.

It is therefore concluded that failure of the batteries is due to softening of the positive active-mass and subsequent failure of the positive plate. From electrical tests, it seems that failure tends to occur first in the central cells of the battery although, at tear-down, all cells exhibit similar evidence of paste softening. This could be related to compression differences through the battery (Because the case was a standard FIAMM automotive case, metal straps were put around the batteries in order to help maintain compression).

From the work undertaken to date, it is thought that the possible reason for this softening may be due to a combination of the following factors.

- The batteries were designed to be under a minimum of 30% compression from the separator. In order to achieve this, and to get the cell groups into the case, it is thought that it would have been necessary to compress the separator with a force as high as 55 kPa. This may have permanently damaged the separator and destroyed its resilience and its ability to maintain an adequate compression on the active material. From the results in Task 6, it is clear that this would have resulted in an early loss of capacity in the battery.
- The charge regime employed was not designed to control the charge factor (the ratio of amount of charge in to that taken out). This meant that as the capacity of the batteries declined cycle by cycle, the amount of overcharge was increasing, further damaging the positive plates.
- In the ECE-15L test, discharge cycling continues until 80% of the original capacity is reached and at this point the battery is re-charged. As the battery declines in capacity from the causes given above, the DoD in the ECE-15L cycling is effectively approaching 100% which, despite the results of Task 7, is considered to be injurious to AGM batteries.

While the original inclination was to attempt to ascertain quickly the cause of failure and then build replacement batteries for further cycling tests, it was subsequently decided that this may not be the correct option. The failure mode appears complex and requires additional work to confirm the reasons. Also, to build new batteries and cycle them could well require a 12-month extension of the Project, which was unlikely to be allowed by the European Commission.

It was therefore agreed to proposed changes to the Work Programme to the Commission which would allow further studies to confirm the reasons for cell failure. It is felt that this will produce valuable information for the industry and enable a positive result to be gained from the Task. With this in mind, the following actions were proposed for the remaining 6 months of the programme.

- Since Sonnenschein have been successful in filling the type G batteries, the units will be parameter tested and, depending on the results, submitted to ECE-15 cycling tests with a controlled charge factor. As these are a different construction (gel) to the type N, S and C batteries, their performance could provide useful information on the failure mode.
- Some spare Type S monoblocks are available and these are to be cycled with a controlled charge factor.
- Separator compression tests are being carried out on a variety of AGM separator materials to determine how they respond to compression under differing loads.
- It is hoped to build and cycle cells constructed from plates from unused FIAMM batteries under different compression levels. Only a limited number of cycles is necessary to confirm the conditions for avoiding early capacity decay.
- Further tear-down analyses are being carried out to confirm that there has been no effect from stray impurities which may have got into the active materials or the electrolyte.
- There is concern that the ECE-15 test is particularly demanding on the lead-acid system—especially the power spike in the cycle and its effect on the negative plate. The opportunity will be taken to test a commercially available battery (the Hawker ‘Genesis’ battery) which has a proven track record in the field. The battery will be set up in two half-strings. One half will be cycled with a ‘good’ recharge regime and the other with a ‘bad’ charge factor. This should give some information as to how the ECE-15 test relates to real performance data and also how battery life can be affected by inadequate control of charging.

The work will be carried out by the existing Partners in Task 9 with assistance from other Partners in the Project and should be completed by the end of 1997.

Task 10. Recycling implications.

A survey into the recycling implications of EV batteries has been commissioned and will be included in the final Project Report. As the additive work has not produced any significant results and as alloy changes are minor, recycling problems are not expected to be significant. There may be some longer-term implications from changes in case design, or materials of construction, in order to maintain compression on the plate stack.

4. Conclusions

This Project has demonstrated that battery companies and suppliers to the industry can work together in pre-competitive research. It seems that the incorporation of conductive additives is unlikely to be the route forward to increased specific energy. On the other hand, improved alloys may enable some further enhancement through more flexibility in battery design.

The work in the various Tasks in this Project has been brought together to produce demonstration batteries for

testing under the Eucar ECE-15L cycling test. While these batteries have experienced early failure, it is hoped that investigations into the causes will yet produce positive information on the requirements for battery design and charging conditions for EV applications.

Acknowledgements

This work has been sponsored jointly by the European members of the Advanced Lead-Acid Battery Consortium together with the European Commission under the Brite–EuRam Programme. Their permission to publish this paper is gratefully acknowledged. This summary of the work has been produced from papers published at the 30th ISATA Meeting held in Florence, Italy, from 16–19 June 1997 and from periodic Project Reports.

References

[1] A. Cooper, J. Power Sources 59 (1996) 161–170.
[2] E. Meissner, H. Döring, H. Clasen, J. Garche, 30th ISATA, Florence, 16–19 June 1997.
[3] J.I. Dyson, A. Turner, C.P. Jones, 30th ISATA, Florence, 16–19 June 1997.
[4] T.A. Robinson, J. Bialacki, G.J. May, 30th ISATA, Florence, 16–19 June 1997.
[5] E. Meissner, E. Bashtevelova, A. Winsell, 30th ISATA, Florence, 16–19 June 1997.
[6] R. Wagner, P. Scharf, 30th ISATA, Florence, 16–19 June 1997.
[7] M.J. Weighall, 30th ISATA, Florence, 16–19 June 1997.
[8] H. Döring, J. Garche, H. Stelzer, H. Tuphorn, 30th ISATA, Florence, 16–19 June 1997.
[9] A. Chabrol, L. Torcheaux, P. Steyer, J.P. Hilger, N. Bui, G. Nouaille-Degorce, L. Albert, 30th ISATA, Florence, 16–19 June 1997.
[10] G. Baudo, H. Döring, N. Kapkov, L. Sella, 30th ISATA, Florence, 16–19 June 1997.